Supplementary methods

Preparation of single cell suspension from the lung

Preparation of single cell suspension from the lung of mice was performed as previously described with modification[1, 2]. Briefly, lung samples were cut into pieces with scissors and put into serum-free RPMI medium supplemented with 100 μg/ml DNase I (Roche applied science) and 50 μg/ml Liberase TM (Roche applied science). After the incubation for 40 min at 37°C, EDTA solution (Nacalai Tesque) was added up to the final concentration of 10 mM, and the samples were further incubated for 10 min at 37°C. After the completion of digestion, samples were subjected to GentleMACS™ Dissociator (Miltenyi biotec), and filtered with 40 μm cell strainer. The filtered samples were centrifuged, and after the removal of supernatant, the cell pellets were treated with ACK solution to remove red blood cells. The treated samples were washed with RPMI medium containing 10% fetal bovine serum, then centrifuged, and pellets were suspended with 30% Percoll solution (GE healthcare). The suspended samples were centrifuged for 20 minutes with 2000 rpm at 20 °C, and the cell pellets were subjected to flow cytometry.

Flow cytometry analysis

For flow cytometry analyses, cells were stained with Ghost Dye Violet 510 reagent (Tonbo Biosciences) according to the manufacturer's instruction to exclude dead cells, and then treated with antibody cocktail solution containing anti-mouse CD16/CD32 (Biolegend) antibody and surface antigen staining antibodies. For the staining of intracellular antigens, after the completion of surface staining, cells were fixed and permeabilized with Lyse/Fix buffer and Perm Buffer I (BD Pharmingen), and stained with antibodies suspended with Perm Buffer III according to the manufacturer's indication. For the staining of human Regnase-1, permeabilized cells were incubated for one hour with anti-human Regnase-1 antibody (1'

antibody, MAB7875, R&D) suspended up to 1:100 volume/volume ratio with staining buffer, then washed with staining buffer and further incubated for one hour with 2' antibody suspended up to 1:100 ratio with staining buffer. Lymphocytes were gated in FSC-A/SSC-A scatter plot as FSC-A^{low} SSC-A^{low} cell population. ILC2s in the lungs of mice were isolated as lineage$^-$ $CD45^+$ $T1/ST2^+$ $Sca\text{-}1^+$ $KLRG1^+$ cells, and human ILC2s were isolated as lineage$^-$$CD45^+$$CRTH2^+$$CD127^+$$CD161^+$ cells (supplementary figures S1B, S6). Lineage markers for mouse included CD4, CD5, CD8a, CD3e, CD19, CD49b, Gr-1, Ter119, CD11b and CD11c. Lineage markers for human included CD3, CD16, CD19, CD14, CD56 and CD20. The antibodies used in this study are listed in supplementary table S11. Data were obtained by using LSRFotessa X-20 (BD Biosciences), and sorting was done with FACSAria III (BD Biosciences). Data were analyzed with FlowJo 10.5.3 software (FlowJo, LLC).

Competitive bone marrow transfer

Lethal irradiation (9 Gy/mouse) was performed on CD45.1 congenic mice with C57BL/6J background, and the mixed bone marrow cells consisted of C57BL/6J background *Regnase-1*$^{-/-}$ mice and CD45.1 congenic mice in 1:1 ratio were by the intravenously injected. The transfered mice were maintained with adding antibiotics (Neomycin 1mg/ml, Polymyxin B 1000 U/ml) into drinking water. Six weeks after reconstitution, the analyses were performed. Each cell type was identified as follows; neutrophils: $GR\text{-}1^+$ $CD11b^{high}$ cells, macrophages: $F4/80^+$ cells, eosinophils: $CD11c^-$ $SiglecF^+$ cells, dendritic cells: $CD11c^+$ MHC class $II^{high}SiglecF^-$ cells, mast cells: $IgE^+C\text{-}kit^+$ cells, basophils: $IgE^+C\text{-}kit^-$ $CD49b^+$ cells, effector/memory $CD4^+$ T cells: $CD4^+$ $TCR\beta^+CD44^+$ cells, naïve $CD4^+$ T cells: $CD4^+TCR\beta^+CD44^-$ cells, effector/memory $CD8^+$ T cells: $CD8^+$ $TCR\beta^+$ $CD44^+$ cells, naïve $CD8^+$ T cells: $CD8^+TCR\beta^+CD44^-$ cells, Th2 cells: $CD4^+CD3^+GATA3^+$ cells, B cells:

$CD19^+$ cells. ILC1s were detected as $lineage^-$ $CD45^+$ IFN-γ^+ lymphocytes and ILC3s were detected as $lineage^-$ $CD45^+$ Rorγt^+ lymphocytes.

t-SNE analysis and clustering

We performed t-distributed stochastic neighbor embedding (t-SNE) analysis on $CD45^+$Linage $^-$ Ghost-dye^- population as reported previously[3] by using FlowJo 10.5.3 (FlowJo, LLC). Events within the gated population was normalized between the mice by using the random down sampling plugin with reducing events up to 1000 events/sample. Then the events in all the samples were combined by concatenating function of FlowJo, and based on the concatenated data we performed the t-SNE analysis. The t-SNE settings were as follows: Iteration 1000, Perplexity 20, Eta 200. Based on the calculated t-SNE scores (X and Y), we performed clustering by using FlowSOM plugin for FlowJo with setting the number of clusters as three[4].

Bleomycin induced pulmonary fibrosis and adaptive transfer of ILC2s

ILC2s were isolated from the lungs of *Regnase-1*$^{-/-}$*Rag2*$^{-/-}$ or control *Rag2*$^{-/-}$ mice as $lineage^-CD45^+T1/ST2^+Sca\text{-}1^+KLRG1^+$ lymphocytes (fig. 1B) One week before the transfer, ex-vivo cultured ILC2s were expanded with 10 ng/ml recombinant mouse IL-2, IL-7 and IL-33 (R&D Systems, Minneapolis, Minnesota). Bleomycin sulfate (Sigma Aldrich, St. Louis, Missouri) was dissolved with PBS, and the solution was intratracheally injected to *Rag2*$^{-/-}$*Il2rg*$^{-/-}$ mice at a dose of 0.15 unit/mouse. The next day, 1.5 x 10^5 ILC2s were intratracheally transferred. The lung samples were collected on day 12 after bleomycin injection. Lung fibrosis was evaluated by using the modified Ashcroft scale [5, 6].

Ex-vivo culture of ILC2s in the lung

The sorted ILC2s were seeded on 96 well u-bottom dish at 5000 cells/well concentration, and cultured with 200 μl of RPMI-1640 medium containing 10% volume/volume fetal bovine serum, 10 mM HEPES, 100 μM nonessential amino acids, 1 mM sodium pyruvate, 100 U/ml penicillin, 100 μg/ml streptomycin, and 50 μM 2-mercaptoethanol supplemented with 10 ng/ml recombinant mouse IL-2 and IL-7 (R&D systems). The supplementation of 10 ng/ml recombinant mouse IL-2 (R&D systems), 10 ng/ml recombinant mouse IL-7 (R&D sytems) and 10 ng/ml recombinant mouse IL-33 (R&D sytems) was done as noted in the manuscript. Culture media was changed three times a week. For the stimulation of ICOS, 3 μg/ml anti-ICOS antibody (clone: C398.4A, Biolegend) was used in reference to the previous study[7].

Hydroxyproline assay

The amount of collagen in the lung tissue was evaluated by hydroxyproline assay (Quickzyme Biosciences) according to the manufacturer's instructions. Briefly, snap-frozen lung tissue (30mg) were homogenized with 300 μl of distiled deionized water. Then, 300 μl of 12M HCl was added, mix well, and heated at 95°C for 20 hours. Next, the samples were cooled up to room temperature, and the samples were centrifuged for 10 min at 13,000g. The supernatant was diluted with 300 μl water. Thirty-five μl of diluted samples were applied to 96-well dish and mixed with 75 μl of assay buffer, incubated for 20 minutes at room temperature, and 75μl of detection reagent was added to the well. After the incubation for 60 minutes at 60°C, the OD value was read at 570 nm.

Histological analysis

Mice were euthanized, and the lung were removed, fixed in Mildform® 10N (FUJIFILM Wako Pure Chemical Corporation, Osaka, Japan), embedded in paraffin, and cut into

4-μm-thick sections. Sections were stained with hematoxylin and eosin and Azan-Mallory.

Lung fibrosis was histologically evaluated by using the modified Ashcroft scale [5, 6]. Briefly, 10 microphotographs were taken from an Azan-Mallory-stained specimen of each mouse lung tissue at 20x magnification. Lung fibrosis of each microphotograph was graded from 0 to 8 by two histologists familiar with lung histopathology (T.T and S.A) and the average score of each mouse lung tissue was calculated.

Multiplex analysis

Culture medium and BALF samples were immediately frozen at -80 ℃ until analysis. Samples were analyzed according to the manufacturer's instructions by using Bio-Plex Pro Mouse Cytokine 23-plex Assay kit (M60009RDPD, Bio-Rad Laboratories) and Bio-Plex 200 system.

Luciferase reporter assay

HEK293 cells were cultured with Dalbecco-Modified Eagle's Medium (Nacalai Tesque) supplemented with 10% fetal bovine serum and 50 μM β-mercaptoethanol (Invitrogen). Regnase-1 WT and D141N mutant expressing plasmids were previously described[8-10]. For the expression of these genes in mammalian cells, pFLAG-CMV2 (SIGMA) was utilized. The 3′UTR sequence of the indicated genes were inserted in firefly luciferase expressing pGL3 promoter plasmid. With each of the constructed pGL3 promoter plasmid, either of plasmid expressing Regnase-1 WT, D141N or empty (control) was transfected simultaneously, and Renilla luciferase expressing plasmid was also transfected as an internal control. Forty-eight hours after the transfection, the cell lysate was subjected to the Dual-Luciferase Reporter Assay system (Promega). Plasmids were transfected into cells by using PEI MAX solution (Polysciences, Inc.) according to the manufacturer's instruction.

RT-qPCR analysis.

Rag2$^{-/-}$ mice were administered with 0.15 U/head bleomycin, and on the day 14 the mice were sacrificed. Mice without bleomycin treatment were used for the control. ILC2s were isolated from the lung by flow cytometry, and were lysed with TRIzol® reagent (Invitrogen). We extracted RNA from the solution, and reverse transcription was performed with ReverTra Ace qPCR RT Master Mix with gDNA remover (Toyobo) according to the manufacturer's instruction. The cDNA fragments were subjected to real-time PCR with SYBR® Green PCR Master Mix (Applied Biosystems), and evaluated by StepOnePlus Real-Time PCR System (Applied Biosystems). The following primer sequences were used: mouse *Actinb*: (forward) 5′- ggctgtattcccctccatcg-3′, (reverse) 5′-ccagttggtaacaatgccatgt-3′, mouse *Regnase-1*: (forward) 5′- cgagaggcaggagtggaaac-3′, (reverse) 5′-cttacgaaggaagttgtccaggctag -3′.

Western blot

Cells were lysed with RIPA buffer. Western blot was performed as described previously[10]. Anti-human Regnase-1 antibody (1' antibody, MAB7875, R&D) and anti-mouse/human β-actin (sc-1615; Santa Cruz) were used. Rabbit anti-mouse/human Regnase-1 antibody was described previously[9]. Luminescence data was obtained by ImageQuant LAS 4000 (GE Healthcare).

RNA sequencing analyses

Isolated ILC2s from competitively transferred mice were lysed with TRIzol (Invitrogen), and total RNA was extracted. The cDNA libraries were prepared by using SMARTer PCR cDNA Synthesis Kit (Clontech) and Nextera DNA Flex Library Prep Kit (Illumina) according to the

manufacturer's instruction, and the samples were sequenced on a HiSeq 2000 system (Illumina). Ribosomal sequences were excluded by using bowtie2 (version 2.2.4), and the reads were mapped on the murine genome (mm10) by using tophat2 (version 2.0.13). After excluding the genes with RPKM value < 10 in both of $CD45.1^+$ ILC2s and $CD45.2^+$ ILC2s, fold changes in count-per-million (CPM) and False Discovery Rate-adjusted *P*-values (FDR-*P*) were calculated by using edgeR with applying quasi-likelihood dispersion estimates[11, 12]. Differentially expressed genes (DEGs) were defined as the genes with FDR- *P* of < 0.05 and fold change of < 0.5 or > 2.0. The Comparative Toxicogenomics Database (CTD) (revision 15822) was used to analyze the associations between human diseases and DEGs[13]. The associations between the upregulated genes and pulmonary diseases was assessed by using "Respiratory Tract Diseases" category in the CTD as a reference. A list of human orthologs of mouse genes was obtained from Ensembl Biomart (version Ensembl Genes 98, GRCm38.p6), and was used to convert mouse genes to their human ortholog counterparts. Pathway analysis was performed using the CGAP BioCarta Pathway in with DAVID 6.8 Bioinformatics Resources[14, 15]..

The accessions for RNA sequencing data is as follows:DNA Data Bank of Japan (DDBJ), accession number: DRA007392.

Prediction of transcription factors associated with the gene sets

The upregulated genes categorized in "Pulmonary fibrosis" by CTD were analyzed with Enrichr[16, 17]. The screening was performed by searching transcription factor binding sites for the genes through referencing the Transfac[18] and JASPAR[19] databases, and transcription factors of mouse were extracted.

Clinical data collection

Clinical information including patients' background, laboratory tests, arterial blood gas analysis, pulmonary function tests and 6MWT at the time of sample collection were obtained. Patients were instructed to visit hospital every 1-3 months to receive chest X-ray, laboratory test and regular interview with physician. Pulmonary function test including FVC, FEV_1 and DLco was performed every 6 months unless contraindications such as pneumothorax was not observed. The median follow-up period was 1674 days for the analysis of peripheral blood and 1241 days for the analysis of BAL, respectively. Progression was defined if any of the following event was observed: > 10% relative decline in FVC, > 15% relative decline in DLco, death or acute exacerbation of IPF. The ratio of ILC2s among lymphocytes in BAL or peripheral blood was determined using flow cytometry (BD LSR Fortessa-X20, BD Bioscience). Human ILC2s were defined as $CD45^+lineage^-CD127^+CRTH2^+CD161^+$ cells (fig. S5). Written informed consent was obtained from all participants.

Clinical sample collection and analysis

BAL was performed according to the guideline[20], and the recovered BALF was centrifuged at 1500 rpm for 5 minutes, then the pellet was stored. Peripheral blood mononuclear cells was prepared by using Ficoll Paque PLUS (GE healthcare) according to the manufacturer's instruction. Cells were suspended with CELLBANKER1 (AMSBIO) and stored at -80°C. BALF lymphocyte fraction or peripheral blood lymphocyte count evaluated as regular practice was multiplied with the ILC2s/lymphocyte ratio, thereby the ratio of BALF ILC2s or the number of peripheral blood ILC2s were calculated.

Statistical analysis

For the analyses of experimental data, either of Microsoft Excel (Microsoft corporation) or GraphPad Prism version 7.00 for Windows (GraphPad Software, La Jolla California USA)

was used, and Student's t-test was performed for the comparisons between the groups.

Statistical analyses for clinical data were performed with EZR (Saitama Medical Centre, Jichi Medical University, Saitama, Japan), which is a graphical user interface for R (The R Foundation for Statistical Computing, Vienna, Austria)[21]. A Fisher's exact test was used for the analysis of categorical variables and Mann Whitney U-test was used for the comparisons of continuous data. The log–rank test was used to evaluate the cumulative survival based on Kaplan-Meyer's curve. To evaluate the power of the cut-off value to detect poor survival, we adopted three-year survival for the calculation, because previous studies reported the median survival of IPF as three years [22-24]. We set the parameters as follows; observation period: 1080 days, the estimated three-year survival of the patients: 0.5, alpha-error: 0.05. We set the survival rate of the patients within each group according to the results of the analysis. The death due to the following reasons were regarded as "Respiratory death": chronic respiratory failure, acute exacerbation of IPF, pneumonia, pneumothorax and lung cancer. For the patients who did not experience any events or whose follow-up was lost, the follow-up period was censored at the day of the last visit. The Cox proportional hazards test was used for the multivariate analysis of survival with a stepwise selection of variables based on the Akaike information criterion. A p value of < 0.05 was considered statistically significant.

Supplementary method references

1. Moro K, Ealey KN, Kabata H, Koyasu S. Isolation and analysis of group 2 innate lymphoid cells in mice. *Nat Protoc* 2015: 10(5): 792-806.

2. Nakatsuka Y, Vandenbon A, Mino T, Yoshinaga M, Uehata T, Cui X, Sato A, Tsujimura T, Suzuki Y, Sato A, Handa T, Chin K, Sawa T, Hirai T, Takeuchi O. Pulmonary Regnase-1 orchestrates the interplay of epithelium and adaptive immune systems to protect

against pneumonia. *Mucosal Immunol* 2018: 11(4): 1203-1218.

3. Cameron GJM, Cautivo KM, Loering S, Jiang SH, Deshpande AV, Foster PS, McKenzie ANJ, Molofsky AB, Hansbro PM, Starkey MR. Group 2 Innate Lymphoid Cells Are Redundant in Experimental Renal Ischemia-Reperfusion Injury. *Front Immunol* 2019: 10(826).

4. Van Gassen S, Callebaut B, Van Helden MJ, Lambrecht BN, Demeester P, Dhaene T, Saeys Y. FlowSOM: Using self-organizing maps for visualization and interpretation of cytometry data. *Cytometry A* 2015: 87(7): 636-645.

5. Ashcroft T, Simpson JM, Timbrell V. Simple method of estimating severity of pulmonary fibrosis on a numerical scale. *Journal of clinical pathology* 1988: 41(4): 467-470.

6. Hübner R-H, Gitter W, Mokhtari NEE, Mathiak M, Both M, Bolte H, Freitag-Wolf S, Bewig B. Standardized quantification of pulmonary fibrosis in histological samples. *BioTechniques* 2008: 44(4): 507-517.

7. Arimura Y, Shiroki F, Kuwahara S, Kato H, Dianzani U, Uchiyama T, Yagi J. Akt is a neutral amplifier for Th cell differentiation. *J Biol Chem* 2004: 279(12): 11408-11416.

8. Matsushita K, Takeuchi O, Standley DM, Kumagai Y, Kawagoe T, Miyake T, Satoh T, Kato H, Tsujimura T, Nakamura H, Akira S. Zc3h12a is an RNase essential for controlling immune responses by regulating mRNA decay. *Nature* 2009: 458(7242): 1185-1190.

9. Iwasaki H, Takeuchi O, Teraguchi S, Matsushita K, Uehata T, Kuniyoshi K, Satoh T, Saitoh T, Matsushita M, Standley DM, Akira S. The IkappaB kinase complex regulates the stability of cytokine-encoding mRNA induced by TLR-IL-1R by controlling degradation of regnase-1. *Nat Immunol* 2011: 12(12): 1167-1175.

10. Mino T, Murakawa Y, Fukao A, Vandenbon A, Wessels HH, Ori D, Uehata T, Tartey S, Akira S, Suzuki Y, Vinuesa CG, Ohler U, Standley DM, Landthaler M, Fujiwara T, Takeuchi O. Regnase-1 and Roquin Regulate a Common Element in Inflammatory mRNAs by

Spatiotemporally Distinct Mechanisms. *Cell* 2015: 161(5): 1058-1073.

11. Robinson MD, McCarthy DJ, Smyth GK. edgeR: a Bioconductor package for differential expression analysis of digital gene expression data. *Bioinformatics* 2010: 26(1): 139-140.

12. McCarthy DJ, Chen Y, Smyth GK. Differential expression analysis of multifactor RNA-Seq experiments with respect to biological variation. *Nucleic Acids Res* 2012: 40(10): 4288-4297.

13. Davis AP, Grondin CJ, Johnson RJ, Sciaky D, McMorran R, Wiegers J, Wiegers TC, Mattingly CJ. The Comparative Toxicogenomics Database: update 2019. *Nucleic Acids Res* 2019: 47(D1): D948-d954.

14. Huang da W, Sherman BT, Lempicki RA. Systematic and integrative analysis of large gene lists using DAVID bioinformatics resources. *Nat Protoc* 2009: 4(1): 44-57.

15. Huang da W, Sherman BT, Lempicki RA. Bioinformatics enrichment tools: paths toward the comprehensive functional analysis of large gene lists. *Nucleic Acids Res* 2009: 37(1): 1-13.

16. Chen EY, Tan CM, Kou Y, Duan Q, Wang Z, Meirelles GV, Clark NR, Ma'ayan A. Enrichr: interactive and collaborative HTML5 gene list enrichment analysis tool. *BMC bioinformatics* 2013: 14: 128.

17. Kuleshov MV, Jones MR, Rouillard AD, Fernandez NF, Duan Q, Wang Z, Koplev S, Jenkins SL, Jagodnik KM, Lachmann A, McDermott MG, Monteiro CD, Gundersen GW, Ma'ayan A. Enrichr: a comprehensive gene set enrichment analysis web server 2016 update. *Nucleic Acids Res* 2016: 44(W1): W90-97.

18. Matys V, Kel-Margoulis OV, Fricke E, Liebich I, Land S, Barre-Dirrie A, Reuter I, Chekmenev D, Krull M, Hornischer K, Voss N, Stegmaier P, Lewicki-Potapov B, Saxel H, Kel AE, Wingender E. TRANSFAC and its module TRANSCompel: transcriptional gene

regulation in eukaryotes. *Nucleic Acids Res* 2006: 34(Database issue): D108-110.

19. Khan A, Fornes O, Stigliani A, Gheorghe M, Castro-Mondragon JA, van der Lee R, Bessy A, Cheneby J, Kulkarni SR, Tan G, Baranasic D, Arenillas DJ, Sandelin A, Vandepoele K, Lenhard B, Ballester B, Wasserman WW, Parcy F, Mathelier A. JASPAR 2018: update of the open-access database of transcription factor binding profiles and its web framework. *Nucleic Acids Res* 2018: 46(D1): D1284.

20. Meyer KC, Raghu G, Baughman RP, Brown KK, Costabel U, du Bois RM, Drent M, Haslam PL, Kim DS, Nagai S, Rottoli P, Saltini C, Selman M, Strange C, Wood B. An official American Thoracic Society clinical practice guideline: the clinical utility of bronchoalveolar lavage cellular analysis in interstitial lung disease. *Am J Respir Crit Care Med* 2012: 185(9): 1004-1014.

21. Kanda Y. Investigation of the freely available easy-to-use software 'EZR' for medical statistics. *Bone Marrow Transplant* 2013: 48(3): 452-458.

22. Raghu G, Rochwerg B, Zhang Y, Garcia CA, Azuma A, Behr J, Brozek JL, Collard HR, Cunningham W, Homma S, Johkoh T, Martinez FJ, Myers J, Protzko SL, Richeldi L, Rind D, Selman M, Theodore A, Wells AU, Hoogsteden H, Schunemann HJ, American Thoracic S, European Respiratory s, Japanese Respiratory S, Latin American Thoracic A. An Official ATS/ERS/JRS/ALAT Clinical Practice Guideline: Treatment of Idiopathic Pulmonary Fibrosis. An Update of the 2011 Clinical Practice Guideline. *Am J Respir Crit Care Med* 2015: 192(2): e3-19.

23. Kim HJ, Perlman D, Tomic R. Natural history of idiopathic pulmonary fibrosis. *Respir Med* 2015: 109(6): 661-670.

24. Richeldi L, Varone F, Bergna M, de Andrade J, Falk J, Hallowell R, Jouneau S, Kondoh Y, Morrow L, Randerath W, Strek M, Tabaj G. Pharmacological management of progressive-fibrosing interstitial lung diseases: a review of the current evidence. *Eur Respir*

Rev 2018: 27(150).

Supplementary figure S1. Competitive bone marrow transfer and Identification of mouse ILC2s

A. Schematic picture for the competitive BM transfer model. **B.** Ratio of a CD45.1$^+$ (WT mice derived) and CD45.2$^+$ (*Regnase-1*$^{-/-}$ mice derived) Th2s in the lung of competitive bone marrow transfer model mice (n = 5).

Supplementary figure S2. Tissue-specificity of Regnase-1-mediated control of ILC2s

Ratio of a CD45.1$^+$ (WT mice derived) and CD45.2$^+$ (*Regnase-1*$^{-/-}$ mice derived) ILC2s in mesenteric fat-associated lymphoid cells (n = 5). Data are shown as mean ± SD. Student's t-test was used for analyses.

Supplementary figure S3. Regnase-1 deficiency affects the number of eosinophils in the lung

Flow cytometry analysis of the population of eosinophils among live cells in *Rag2*$^{-/-}$ mice and *Regnase-1*$^{-/-}$ *Rag2*$^{-/-}$ mice.

Supplementary figure S4. The characterization of *Regnase1*-deficient ILC2s

Cell surface expression levels of the indicated proteins on the ILC2s in the lung of *Rag2*$^{-/-}$ and *Rag2*$^{-/-}$ *Regnase1*$^{-/-}$ mice (n = 5). Expression levels were evaluated by flow cytometry. Data are shown as mean ± SD. Student's t-test was used for analyses. MFI: mean fluorescence intensity.

Supplementary figure S5. *Regnase1*-deficient ILC2s promote pulmonary fibrosis

A. Top 15 human diseases that were associated with the human ortholog counterparts of

upregulated genes. Comparative Toxicogenomics Database (CTD) analyzer was utilized for the analysis. **B.** Schematic figure of the adaptive transfer of ILC2s into bleomycin-induced pulmonary fibrosis model mice. ILC2s sorted from the lungs of *Rag2*$^{-/-}$ mice or *Regnase-1*$^{-/-}$ *Rag2*$^{-/-}$ mice were cultured in the presence of 10 ng/ml IL-2 and IL-7 for 7 to 14 days, then expanded in the presence of 10 ng/ml IL-2, IL-7 and IL-33 for 7 days. On the day following intratracheal injection of 0.15 unit/head bleomycin, 1.5 x 10^5 cultured ILC2s were intratracheally transferred, and the samples were collected on day 12.

Supplementary figure S6. Identification of human ILC2s

Representative gating strategy picture for human ILC2s by flow cytometry. Human ILC2s were identified as CD45$^+$Lineage$^-$CRTH2$^+$CD161$^+$IL-7R$^+$ cells. Doublet depletion was done by the analysis of FSC-A/FSC-H and SSC-A/SSC-H.

Supplementary figure S7. Evaluation of human Regnase-1 protein by flow cytometry

A. Western blot for the cell lysate prepared from WT and *Regnase-1*-deficient Jurkat cells using anti-human Regnase-1 antibody MAB7875. The red arrow indicates the signal for Regnase-1. **B.** Flow cytometry histogram (upper) and dot plot (lower) comparing the fluorescence intensity between WT (red) and *Regnase-1*-deficient (blue) Jurkat cells. **C.** Flow cytometry histogram (upper) and dot plot (lower) comparing the fluorescence intensity between human peripheral blood ILC2s treated with primary antibody (MAB7875) plus secondary antibody (red) and secondary antibody only (blue).

Supplementary figure S8. Regnase-1 expression negatively correlates with the ILC2 number in human BAL.

Correlation between the number of ILC2s among the BAL cells and Regnase-1 protein

expression levels of ILC2s in BAL measured by flow cytometry. Spearman's rank correlation test was used for analysis.

Supplementary figure S9. The clinical significance of ILC2 number in peripheral blood of in IPF patients

A. The associations between ILC2 number in peripheral blood and the indicated plasma cytokine levels in IPF patients. Spearman's rank correlation test was used for analysis. **B.** A Receiver Operating Curve was drawn to determine the optimal cutoff value of the number of ILC2s in peripheral blood to identify IPF patients who died due to respiratory causes. The area under the curve was 0.645. Several values were tested, and 1557 cells/ml was determined to be the cutoff value.

Supplementary figure S10. A graphical summary of the findings in this study

Regnase-1 expressed in ILC2s in the lung of mice suppresses the expression of ICOS, GATA3 or EGR-1 through the destabilization of the mRNAs coding these proteins, thereby restrict the proliferation and the expression of genes associated with pulmonary fibrosis. Also in human, the decrease in Regnase-1 protein levels correlated with the increase in ILC2 population in BAL, and the increased number of ILC2s was an independent factor for worse survival in IPF patients. These data suggest that Regnase-1 inhibits promotion of lung fibrosis by suppressing pro-fibrotic function of ILC2s both in mouse and human.

Supplementary figure S1

A

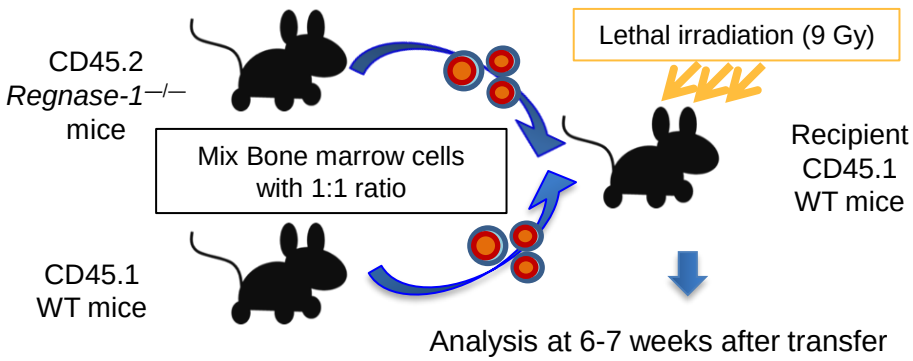

B

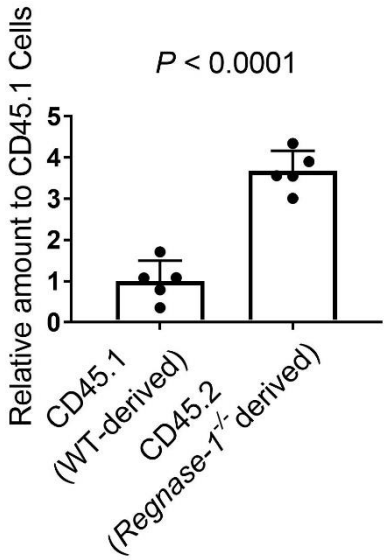

Supplementary figure S2

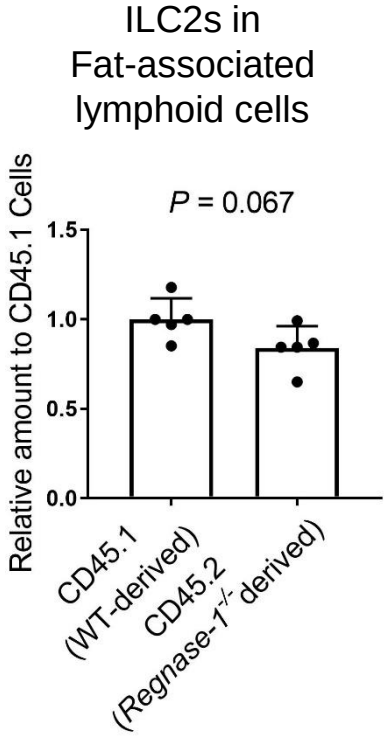

Supplementary figure S3

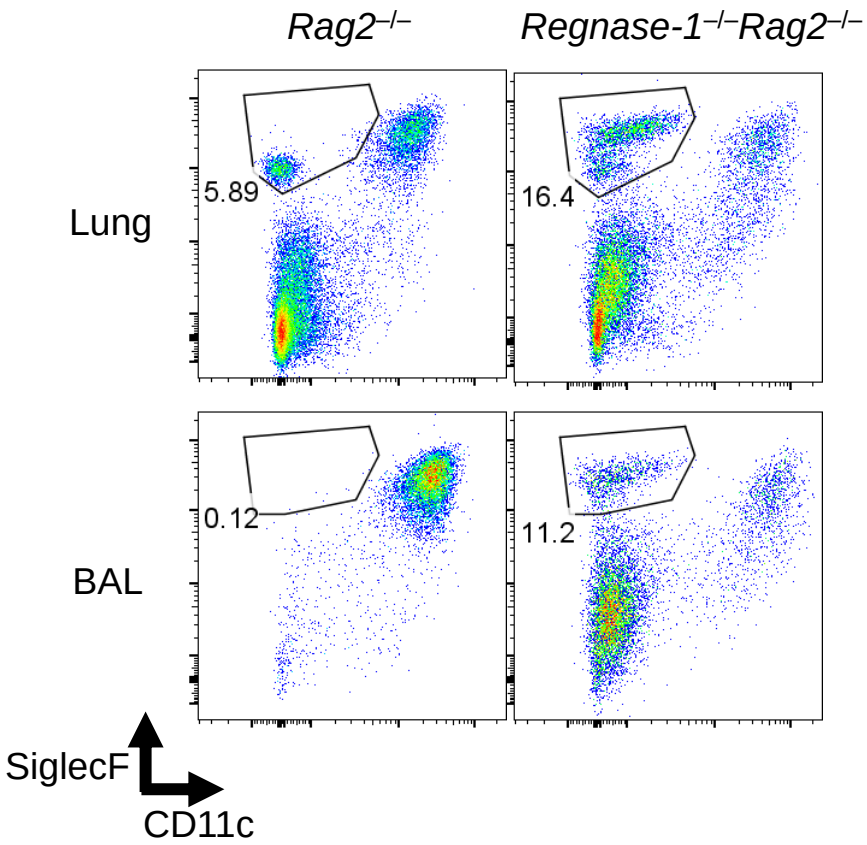

Supplementary figure S4

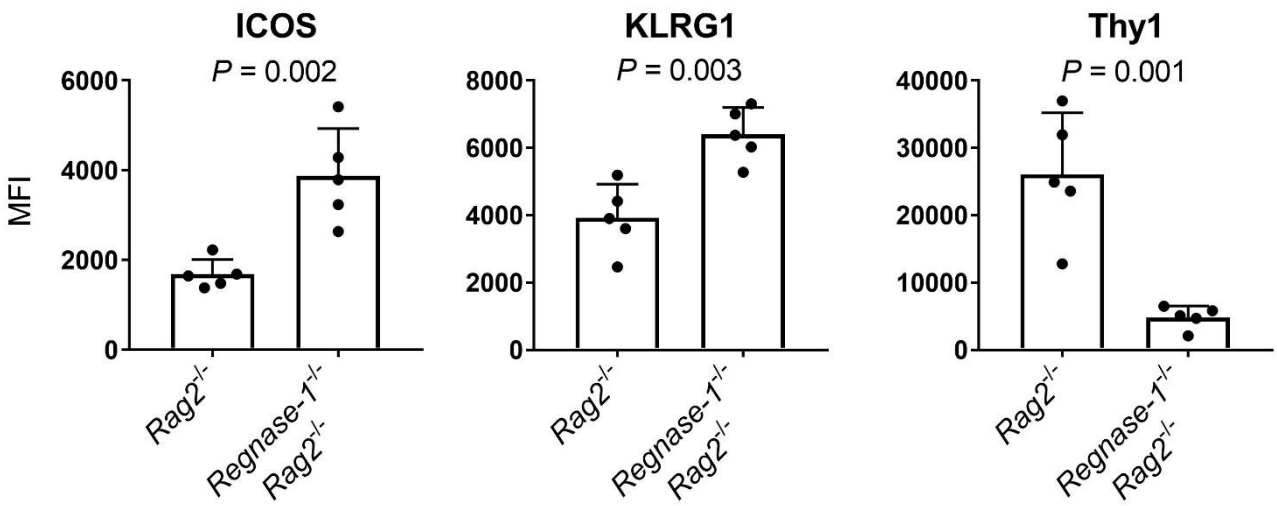

Supplementary figure S5

A

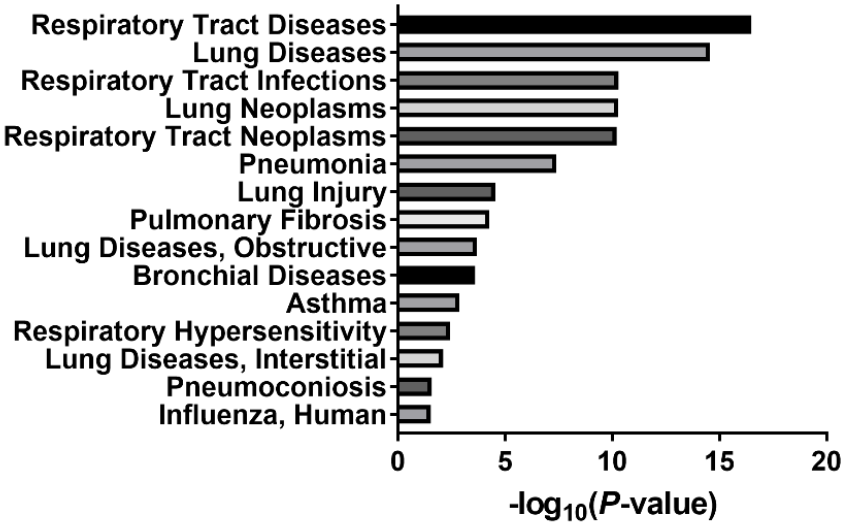

B

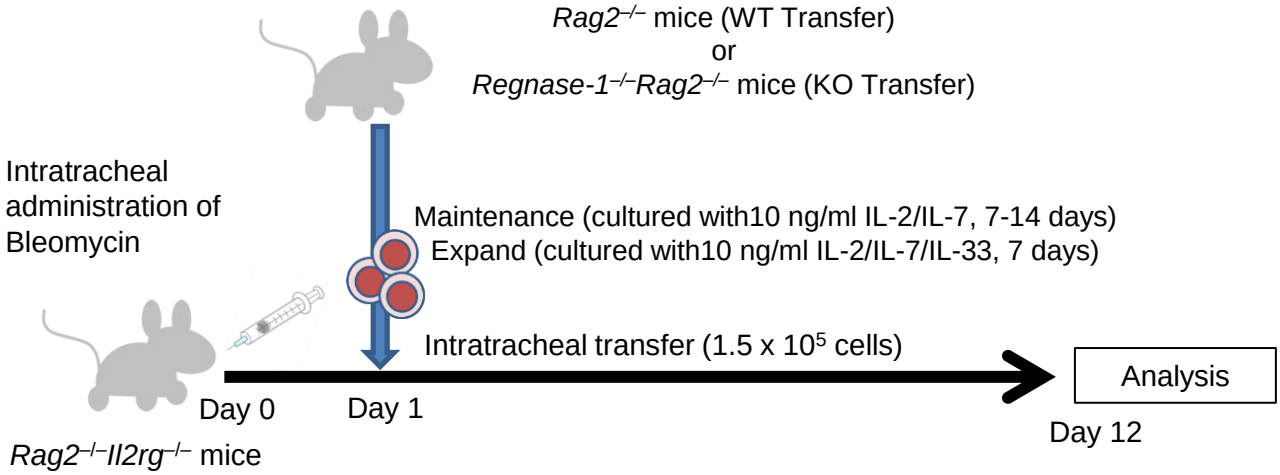

Supplementary figure S6

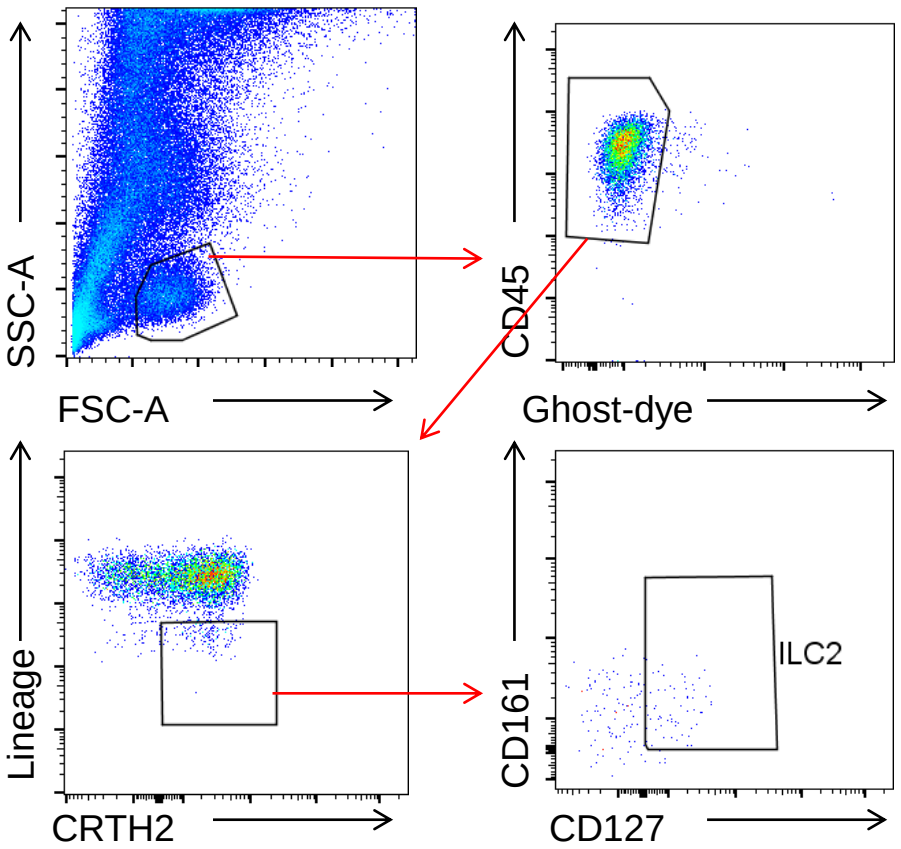

Supplementary figure S7

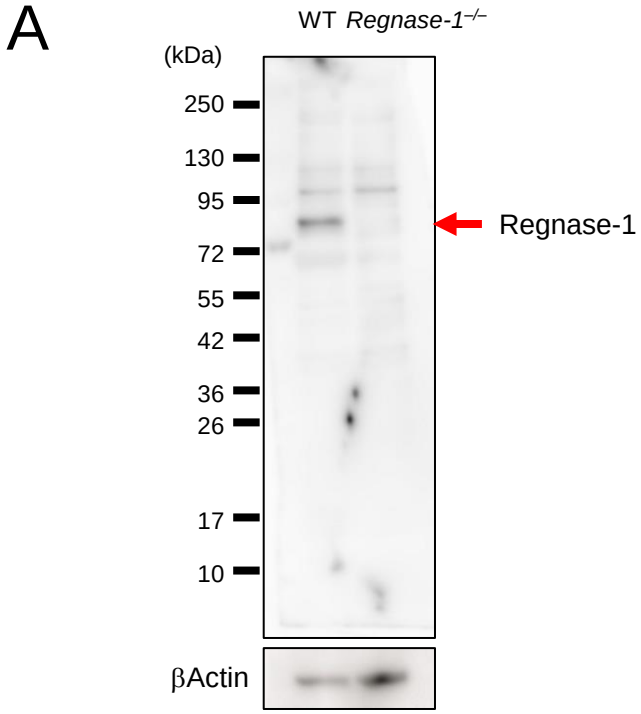

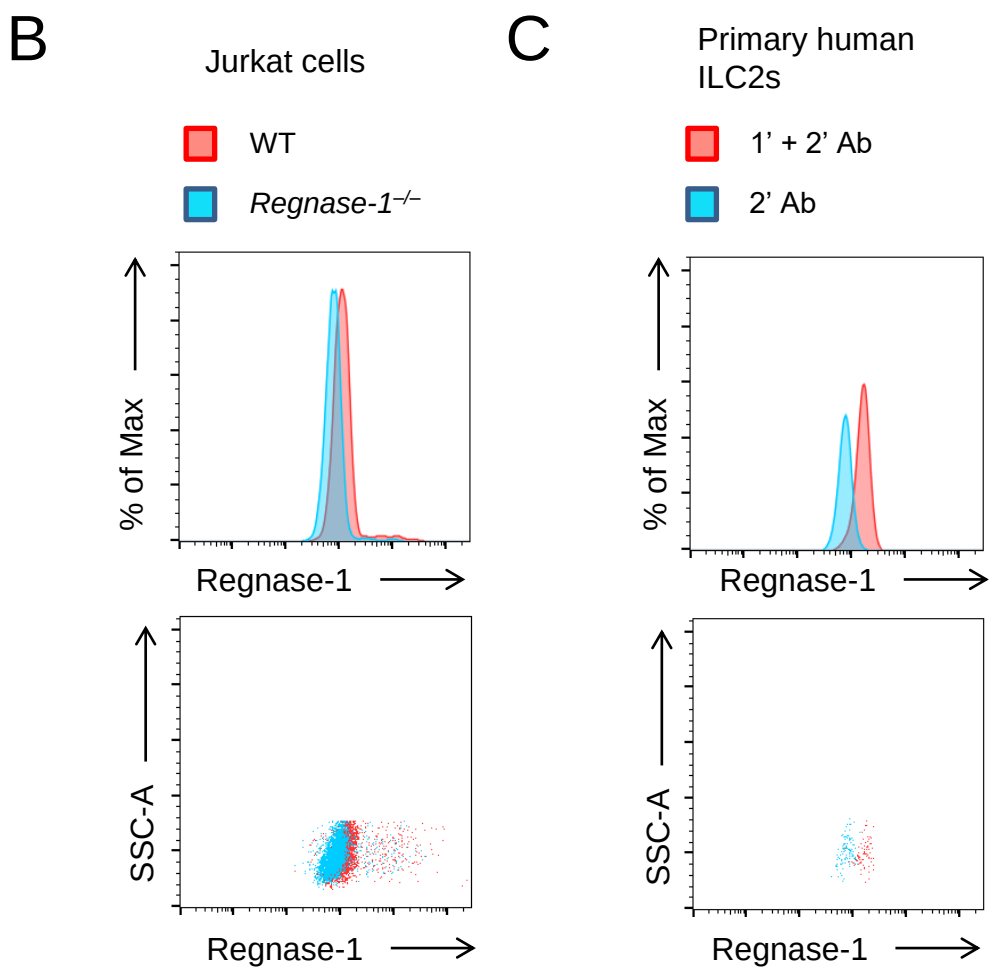

Supplementary figure S8

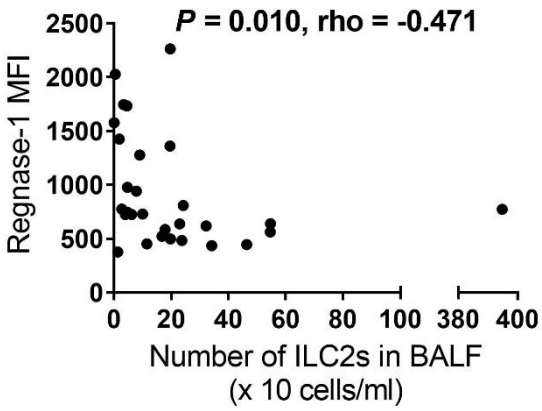

Supplementary figure S9

A

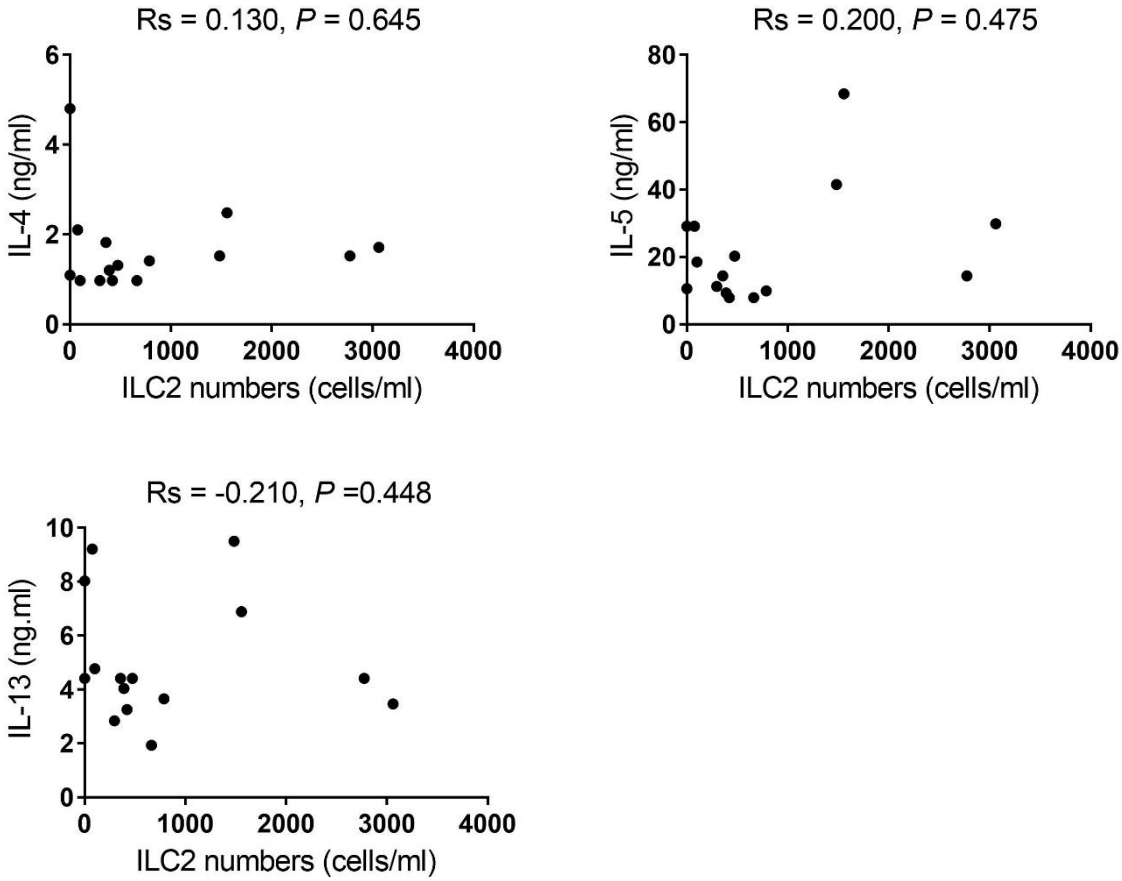

B

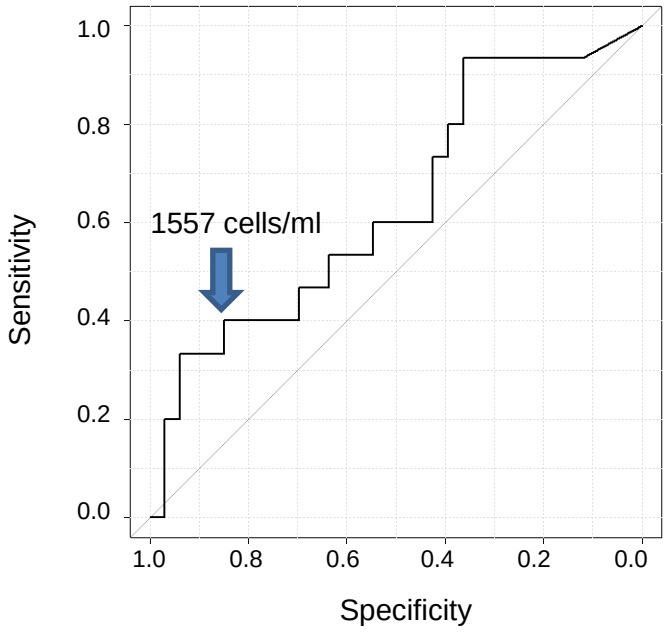

Supplementary figure S10